

SHAPE-RESONANCE-ENHANCED NUCLEAR MOTION EFFECTS IN ELECTRON-  
MOLECULE SCATTERING AND MOLECULAR PHOTOIONIZATION

by

J. L. Dehmer and Dan Dill

MASTER

Prepared for  
International Conference  
on the  
Physics of Electronic and Atomic Collisions  
Kyoto, Japan  
August 29, 1979 - September 4, 1979

CONFIDENTIAL  
This document contains information which is classified as CONFIDENTIAL under Executive Order 11652, dated 5/11/64, and is to be controlled in accordance with the provisions of that order. It is to be distributed only to those individuals who are authorized to receive it. It is to be destroyed when it is no longer needed for the purpose for which it was prepared.



U of C-AUA-USDOE

**ARGONNE NATIONAL LABORATORY, ARGONNE, ILLINOIS**

**Operated under Contract W-31-109-Eng-38 for the  
U. S. DEPARTMENT OF ENERGY**

**DISTRIBUTION OF THIS DOCUMENT IS UNLIMITED**

# SHAPE-RESONANCE-ENHANCED NUCLEAR MOTION EFFECTS IN ELECTRON- MOLECULE SCATTERING AND MOLECULAR PHOTOIONIZATION\*

J. L. Dehmer

Argonne National Laboratory, Argonne, Illinois 60439 U.S.A.

and

Dan Dill

Department of Chemistry, Boston University, Boston, Massachusetts 02215 U.S.A.

Shape resonances in the electronic continuum of molecules induce strong coupling between vibrational and electronic motion over a spectral range much broader than the resonance half width. In photoionization, this coupling causes large deviations from Franck-Condon intensity distributions and strong dependence of photoelectron angular distributions on the vibrational state of the residual ion. In electron scattering, it enhances vibrational excitation. We review recent work in which new, observable manifestations of this coupling have been predicted theoretically and then verified experimentally.

## INTRODUCTION

Shape resonances are now widely recognized as a powerful and broadly applicable tool for the study of the dynamics of the electronic continuum of molecules: They are being identified in the photoionization ( $h\nu + M$ ) and electron scattering ( $e + M$ ) spectra of a growing and diverse collection of molecules, and are expected to occur somewhere in the spectra of most (non-hydride) molecules. Owing to their localized nature, such resonances often produce intense spectral features; and, in many circumstances, their well-defined  $l$  character is directly reflected in angular distributions. Moreover, their one-electron nature lends itself to study by a realistic, independent-electron theoretical method such as the multiple-scattering model<sup>1,2</sup> (MSM) used here, with the concomitant flexibility in terms of molecular systems, energy ranges, and alternative physical processes. The purpose of the present article is to emphasize another facet of shape resonances—their interaction with vibrational motion—which once again traces to their localized nature. Recent theoretical work,<sup>3,4</sup> employing the MSM in the adiabatic nuclei approximation, has predicted several observable consequences of this coupling and has led to experimental verification<sup>5,6</sup> and the expectation of numerous similar observations in the future.

We will stress the unifying aspects of shape-resonance-enhanced nuclear motion effects in  $e + M$  and  $h\nu + M$  systems; however, as they do manifest themselves differently, we will introduce them separately: Molecular photoionization at wave-

\*Work performed under the auspices of the U.S. Department of Energy and National Science Foundation Grant CHE78-08707. Acknowledgement is also made to the Donors of the Petroleum Research Fund, administered by the American Chemical Society, for partial support of this work.

lengths unaffected by autoionization, predissociation, or ionic thresholds is generally believed to produce Franck-Condon (FC) vibrational intensity distributions and  $v$ -independent photoelectron angular distributions. We will show that a major breakdown of this picture occurs in the vicinity of a shape resonance. In particular, the temporary trapping of the photoelectron by a centrifugal barrier enhances the coupling between electronic and vibrational motion, leading to striking non-FC intensities and strongly  $v$ -dependent asymmetry parameters over a broad spectral range encompassing the resonance. We illustrate these ideas with a calculation<sup>4</sup> of the  $3\sigma_g$  photoionization channel of  $N_2$ , which exhibits the well-known  $\sigma_u$ ,  $f$ -wave shape resonance (see, e.g., Refs. 2, 4, 7-21). In addition to predicting non-FC vibrational branching ratios, we account for the long unexplained observation<sup>22-27</sup> that the  $\beta$  values for production of  $N_2^+ X^2\Sigma_g^+$  ( $v=0, 1$ ) differ significantly at 584 Å (and other wavelengths). Very recently experimental measurements<sup>6</sup> on the analogous  $5\sigma$  channel in CO have verified the non-FC vibrational intensity distributions predicted by this picture. Unpublished theoretical work<sup>28</sup> on  $CO_2$  and experimental work<sup>29</sup> on  $N_2$  will also be summarized. We believe these illustrations are merely the first of many examples of equivalent effects that have hitherto gone undetected only because vibrationally-resolved photoelectron studies have not been carried out systematically through molecular shape resonances, as is now possible with synchrotron radiation sources.

The connection between shape resonances in  $e+M$  and  $h\nu+M$  systems is not completely obvious since the two have different numbers of electrons. Nevertheless, as discussed in more detail elsewhere,<sup>30</sup> a similar manifold of resonances occurs in the two cases for the same target molecule, except that those in  $e+M$  are shifted 5 to 15 eV to higher electron energy relative to those in  $h\nu+M$ . The similarity arises because the shape resonances are localized in the molecular core where the potential is dominated by the nuclei and those electrons common to both  $h\nu+M$  and  $e+M$ . The shift reflects the additional repulsion caused by the extra electron in  $e+M$ . For the purposes of discussion, it is convenient to define two energy ranges for  $e+M$ . In the low-energy ( $< 10$  eV) portion of the spectrum, the importance of shape resonances is widely appreciated.<sup>31-33</sup> The  $\pi_g$   $d$ -wave ( $l=2$ ) resonance at 2.4 eV in  $e-N_2$  scattering is perhaps the most thoroughly studied example (see, e.g., Refs. 2, 31-44). Shape resonances in this energy region are related to highly localized states in the discrete portion of the  $h\nu+M$  system. They stand out clearly above the nonresonant background, have widths on the order of an eV, and are usually dominated by a single asymptotic angular momentum, which imposes a well-defined angular distribution characteristic of that  $l$ . Recently we have focussed attention on another class of shape resonances,<sup>3</sup> falling in the intermediate-energy (10-40 eV) range. These quasi-bound states are related to those resonances lying in the  $h\nu+M$  continuum and have emerged in the course of our current survey studies of electron-molecule scattering using the MSM. Compared to their low-energy counterparts, these resonances are broader, are usually barely detectable in the elastic or total scattering cross sections, and often are composed of significant contributions from several asymptotic angular momenta, whose mixture can vary significantly within the resonance. These properties are consistent with the picture of a quasi-bound state lying near the top of its centrifugal barrier. These weak resonances are, however, very sensitive to changes in the molecular geometry and can therefore couple significantly to nuclear motion. We have found<sup>2, 3, 45</sup> that these features are thereby enhanced in vibrational excitation and appear prominently, all the more so because the nonresonant background is negligible in the vibrationally inelastic channels. Experimental evidence

is sparse, possibly because shape-resonant structure in the 10-40 eV range was not expected and measurements were concentrated instead in the low-energy range. Several years ago, Pavlovic et al.<sup>46</sup> reported a broad enhancement in e-N<sub>2</sub> vibrational excitation in the 15-35 eV range. We have shown<sup>45</sup> that this corresponds to a  $\sigma_u$  shape-resonant enhancement, centered at 26 eV in our MSM calculation, and that it is mainly f-wave in character, though with non-negligible mixtures of  $\ell = 1, 5$ . We have also carried out MSM calculations<sup>3</sup> of e-CO<sub>2</sub> scattering in which we observed multiple intermediate-energy resonances. Here we show that two of these, the  $\sigma_g$  and  $\sigma_u$  resonances at 13.5 eV and 29.5 eV, respectively, lead to significant excitation of the symmetric-stretch mode in CO<sub>2</sub>. Prompted by these predicted enhancements, Tronc, Azria, and Paineau<sup>5</sup> have searched for and just confirmed enhanced symmetric-stretch excitation in e-CO<sub>2</sub> at 11 eV and 29.5 eV. Further work<sup>47</sup> has located analogous enhancements in e-CO scattering at 19.5 eV which one would expect on the basis of the e-N<sub>2</sub> results. As in the case of  $h\nu + M$ , we believe that these prototype studies are but the tip of the iceberg.

## FUNDAMENTALS

The enhanced coupling between nuclear and electronic modes arises from the quasi-bound nature of the shape resonant state, which is localized in a spatial region of molecular dimensions by a centrifugal barrier. This barrier, and, hence, the energy and lifetime (width) of the resonance are sensitive functions of internuclear separation  $R$  and vary significantly over a range of  $R$  corresponding to the ground state vibrational motion. We will illustrate this with an example from molecular photoionization, although we emphasize that the illustration would be very similar for electron-molecule scattering. In the upper-left portion of Figure 1, the dashed curves represent separate, fixed- $R$  calculations<sup>4</sup> of the partial cross sections for N<sub>2</sub>  $3\sigma_g$  photoionization over the range  $1.824 a_0 \leq R \leq 2.324 a_0$ , which spans the N<sub>2</sub> ground state vibrational wave function. The peak in the  $3\sigma_g$  partial cross section curves is caused by the shape resonance in the  $\sigma_u$  ionization channel. This resonance has been studied extensively<sup>2, 4, 7-21</sup> in inner-shell, valence-shell, and oriented-molecule contexts and is known to result from a centrifugal barrier acting on the f-wave ( $\ell = 3$ ) component of the  $\sigma_u$  final-state wave function. Of central importance in Figure 1 is the clear demonstration that resonance positions, strengths, and widths are sensitive functions of  $R$ . In particular, for larger separations, the effective potential acting on the  $\ell = 3$  component of the  $\sigma_u$  wave function is more attractive and the shape resonance shifts to lower kinetic energy, becoming narrower and higher. Conversely, for lower values of  $R$ , the resonance is pushed to higher kinetic energy and is weakened. This indicates that nuclear motion exercises great leverage on the spectral behavior of shape resonances, since small variations in  $R$  can significantly shift the delicate balance between attractive (mainly Coulomb) and repulsive (mainly centrifugal) forces which combine to form the barrier. In the present case, variations in  $R$  corresponding to the ground state vibration in N<sub>2</sub> produce significant resonant behavior over a spectral range several times the FWHM of the resonance calculated at  $R = R_g$ . By contrast, non-resonant channels are relatively insensitive to such variation in  $R$ , as will be shown by our results on the  $1\pi_u$  and  $2\sigma_u$  photoionization channels in N<sub>2</sub>, to be published elsewhere.<sup>48</sup>

Thus, in the vicinity of a shape resonance in photoionization, the electronic transition moment varies rapidly with  $R$ , indicating strong coupling between electronic and vibrational motion. In the adiabatic nuclei approximation,<sup>49</sup> the effects of

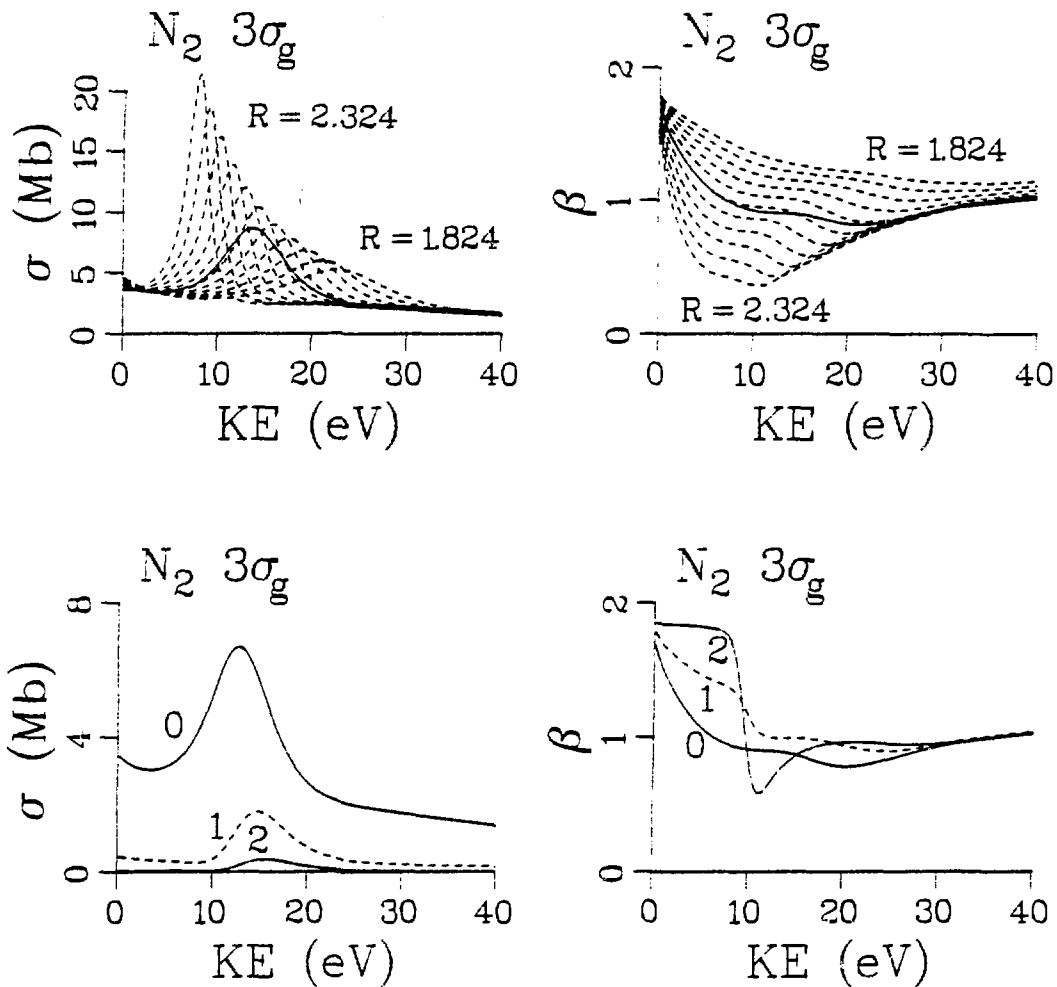


Figure 1. Cross sections  $\sigma$  and asymmetry parameters  $\beta$  for photoionization of the  $3\sigma_g(v_1=0)$  level of  $N_2$ . Top: Fixed  $R$  (----) and  $R$ -averaged, vibrationally unresolved (—) results. Bottom: Results for resolved final-state vibrational levels,  $v_f=0-2$ .

this coupling can be estimated by computing the net transition moment for a particular vibrational channel as an average of the  $R$ -dependent dipole amplitude, weighted by the product of the initial- and final-state vibrational wave functions at each  $R$ :

$$D_{v_f v_i}^- = \int dR \chi_{v_f}^\dagger(R) D^-(R) \chi_{v_i}(R) . \quad (1)$$

The vibrational wave functions are approximated by harmonic oscillator functions in the results reported below, and the "minus" denotes that incoming-wave boundary conditions have been applied.<sup>1,2,9</sup> This "coupled" complex dipole amplitude is converted to partial cross sections and photoelectron angular distributions using standard formulae.<sup>1,2,9</sup>

For electron-molecule scattering, the coupling can be treated in an analogous way by folding the R-dependent T-matrix elements with the initial and final vibrational wave functions. The resulting electronically-elastic cross section formula is<sup>3, 49</sup>

$$\sigma_{f \leftarrow i} = \pi \left( \frac{E_f}{E_i} \right)^{1/2} E_i^{-1} \sum_{\ell m, \ell' m'} \left| \int dR \chi_{v_f}^\dagger(R) T_{\ell m, \ell' m'}(R) \chi_{v_i}(R) \right|^2, \quad (2)$$

where  $T_{\ell m, \ell' m'}(R)$  is the R-dependent element of the body-frame T matrix in angular momentum basis, and  $E_i$  and  $E_f$  are the electron kinetic energy before and after the collision. The integral in Eq. (2) is equivalent to Eq. (1), only now the vibrational wave functions belong to a single electronic state of the target molecule, since we neglect electronic transitions in this work.

Before discussing the observable consequences of the coupling represented in Eqs. (1) and (2), two points should be noted. First, these expressions are generalized to arbitrary molecular geometry by substituting normal-coordinates  $Q_j$  in place of R, though interaction between normal modes could be a complicating feature. Second, significant non-adiabatic effects are expected when the lifetime of the resonance and the vibrational period are comparable. Examples of this are known for low-energy electron molecule scattering, e.g., the 2.4 eV  $\pi_g$  resonance in  $N_2$ ,<sup>35, 37</sup> where non-adiabatic effects induce modulations on the resonance profile.

## PHOTOIONIZATION RESULTS

Effects of nuclear motion on individual vibrational channels in photoionization are shown in the bottom half of Figure 1. Looking first at the partial cross sections, we see that the resonance position varies over a few volts depending on the final vibrational state, and that higher levels are relatively more enhanced at their resonance position than is  $v_f=0$ . This sensitivity to  $v_f$  arises because transitions to alternative final vibrational states preferentially sample different regions of R. In particular,  $v_f=1, 2$  sample successively smaller R, governed by the maximum overlap with the ground vibrational state, causing the resonance in those vibrational channels to peak at higher energy than that for  $v_f=0$ . The impact of these effects on branching ratios is clearly seen in Figure 2, where the ratio of the higher  $v_f$  intensities to that of  $v_f=0$  is plotted in the resonance region. There we see the ratios, slightly above the FC factors<sup>50</sup> (9.3%,  $v_f=1$ ; 0.6%,  $v_f=2$ ) at zero kinetic energy, go through a minimum just below the resonance energy in  $v_f=0$ , then increase to a maximum as individual  $v_f > 0$  vibrational intensities peak, finally approaching the FC factors again at high kinetic energy. Note the maximum enhancement over the FCFs is progressively more pronounced for higher  $v_f$ , i.e., 340% and 1300% for  $v_f=1, 2$ , respectively. Gardner and Samson<sup>51</sup> have systematically measured vibrational intensity distributions in  $N_2$ ; however, the discrete wavelengths utilized in that study did not cover the critical kinetic energy range between 10 and 25 eV. Their data show non-FC effects but these were believed to be due mainly to autoionization. It may be significant that their 584 Å and 537 Å ( $v_f=1$ )/( $v_f=0$ ) ratios were 6.9%, i.e., lower than the FCF, and that the 304 Å ratio was 13.1%, i.e., higher than the FCF; however, this is not conclusive. A systematic mapping of the critical region in Figure 2 using synchrotron radiation is needed to test the prediction given here.

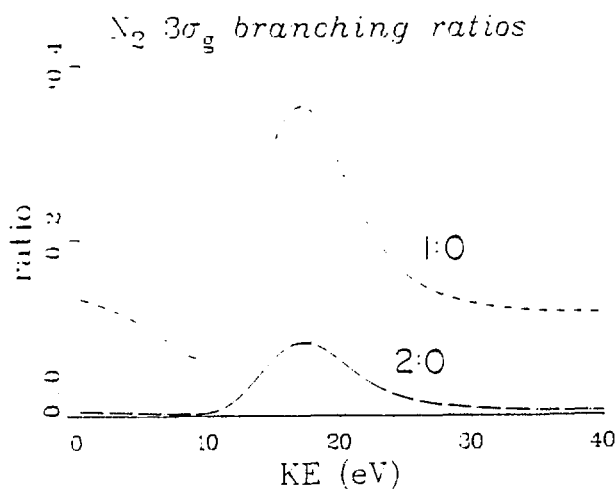


Figure 2. Vibrational state branching ratios  $\sigma(v_f)/\sigma(v_f=0)$  for photoionization of the  $3\sigma_g$  level of  $N_2$ .

Even when the final vibrational levels  $v_f$  of the ion are unresolved (summed over), vibrational motion within the initial state  $v_f=0$  causes Eq. (1) to yield results significantly different from the  $R=R_e$  result, because the  $R$  dependence of the shape resonance is highly asymmetric. This gross effect of  $R$  averaging can be seen in the upper half of Figure 1 by comparing the solid line ( $R$ -averaged result, summed over  $v_f$ ) and the middle dashed line ( $R=R_e$ ). Hence, even for the calculation of gross properties of the whole, unresolved electron band, it is necessary to take into account vibrational motion effects in channels exhibiting shape resonances. As we stated earlier, this is generally not a critical issue in non-resonant channels.

Equally dramatic are the effects on  $\beta(v_f)$  shown in the lower right-hand portion of Figure 1. Especially at and below the resonance position, the  $\beta$ 's vary greatly for different final vibrational levels. The  $v_f=0$  curve agrees well with the solid curve in the upper half, since the gross behavior of the vibrationally unresolved electronic band will be governed by the  $\beta$  of the most intense component. The  $R=R_e$  curve has been found to agree well with recent wavelength-dependent measurements,<sup>20,21</sup> and the agreement is improved by the slight damping caused by  $R$  averaging. More significant for the present purposes is the  $v_f$  dependence of  $\beta$ . Carlson first observed<sup>22,23</sup> that, at  $584 \text{ \AA}$ , the  $v_f=1$  level in the  $3\sigma_g$  channel of  $N_2$  had a much larger  $\beta$  than the  $v_f=0$  level even though there was no apparent autoionizing state at that wavelength. This has been studied in the meantime by several workers<sup>24-27</sup> with the same general conclusions, i.e.,  $\beta(v_f=0) \sim 0.7$  and  $\beta(v_f=1) \sim 1.4$ . This is in semiquantitative agreement with the present calculation which gives  $\beta(v_f=0) \sim 1.0$  and  $\beta(v_f=1) \sim 1.5$ . Although the agreement is not exact, we feel this demonstrates the "anomalous"  $v_f$ -dependence of  $\beta$  in  $N_2$  stems mainly from the  $\sigma_u$  shape resonance which acts over a range of the spectrum many times its own  $\sim 5 \text{ eV}$  width. The underlying cause of this effect is the shape-resonance-enhanced  $R$  dependence of the dipole amplitude, just as for the vibrational partial cross sections. In the case of  $\beta(v_f)$ , however, both the  $R$  dependence of the phase and of the magnitude of the complex dipole amplitude play a crucial role, whereas the partial cross sections depend only on the magnitude.

Shortly after the theoretical work described above was completed, Stockbauer et al.<sup>6</sup> confirmed the prediction of striking non-FC vibrational intensity distributions by measuring vibrational branching ratios for the analogous  $\sigma$  shape resonance in the

5 $\sigma$  photoionization channel of CO using synchrotron radiation from the National Bureau of Standards SURF-II storage ring. Their results are presented in Figure 3 as ratios of intensities of the  $v=1, 2,$  and  $3$  levels of  $\text{CO}^+ X^2\Sigma^+$  to that of the ground vibrational state of the ion, as functions of incident photon energy. Immediately apparent in Figure 3 is that, aside from the structures at  $\sim 19.5$  eV to be discussed later, the gross pattern of spectral variation of these ratios strongly resembles that described above for the analogous states in  $\text{N}_2$ . Specifically, the  $(v=1)/(v=0)$  curve shows an oscillation with a minimum at  $\sim 21.4$  eV and a maximum at  $\sim 22.3$  eV and a peak-to-trough ratio of  $\sim 3$ . The  $(v=2, 3)/(v=0)$  curves are less well defined but clearly show successively greater enhancement at  $\sim 22$  eV, relative to their weak background levels. Accordingly, these experimental results were interpreted as the first direct observation of the effects of shape resonances on vibrational intensity distributions. Note that the enhancement in the ratios centered at  $\sim 19.5$  eV is far removed from the resonance position<sup>14</sup> ( $\sim 24$  eV), does not fit into the simple pattern predicted by theory, and is very likely due to unresolved autoionization structure<sup>52</sup> (converging to  $\text{CO}^+ B^2\Sigma^+$  at 19.7 eV) in that portion of the spectrum. A large number of autoionization structures have also been observed<sup>53</sup> throughout the 22-26 eV region; however, these are extremely weak, doubly-excited features, and are not expected to significantly affect the present results, which are dominated by one-electron excitations.

Significant differences are also observed between the experimental results for CO and the theoretical results<sup>4</sup> for  $\text{N}_2$ . For example, the resonance maxima of the excited vibrational levels in Figure 3 are near 22 eV or approximately 2 eV below the reported position of the shape resonance in the vibrationally unresolved 5 $\sigma$  band, which is dominated by the  $v=0$  vibrational channel. As noted earlier,

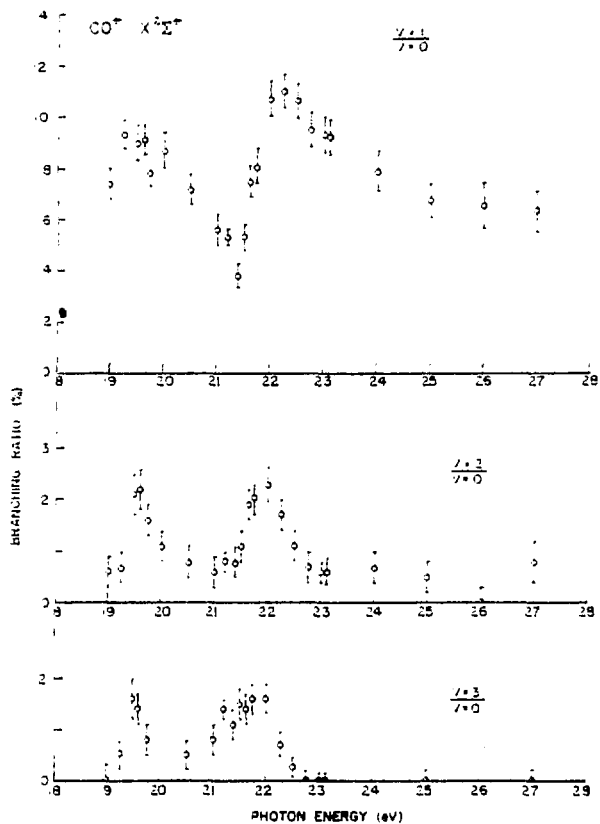


Figure 3. Photoionization branching ratios for the  $v=0-3$  levels of  $\text{CO}^+ X^2\Sigma^+$ .



in  $N_2$  the resonances in the vibrationally excited levels fall  $\sim 2$  eV above the resonance in the unresolved band. We believe this reflects the differences in relative positions of the electronic potential energy curves for the two molecular systems. To see this, we note that in the  $R$ -dependent calculations for  $N_2$  photoionization, the  $\sigma_u$  shape resonance shifts to lower energy and becomes narrower when  $R$  is increased and shifts to higher energy and broadens when  $R$  is decreased. In  $N_2$ ,  $R_e$  for the  $X^2\Sigma_g^+$  ionic state is slightly larger than that for the  $X^1\Sigma_g^+$  neutral state, having the effect of preferentially weighting the low- $R$  portion of the FC region. As a consequence, the resonances in  $v=1$  and 2 are shifted to higher energy than in  $v=0$ . In CO, the  $R_e$  of the  $X^2\Sigma^+$  ionic state is slightly smaller than that of the  $X^1\Sigma^+$  neutral state, so the observed opposite shift would appear consistent with the above argument. A calculation on CO would test this tentative interpretation. Another contrast is observed between the absolute values of the ratios in Figure 3 and those reported<sup>4</sup> for  $N_2$ . For example, in the CO case the  $(v=1)/(v=0)$  ratio is everywhere higher than the FCF (3.8%),<sup>50</sup> except at the minimum at  $\sim 21.4$  eV where the experimental curve dips near the FCF. In  $N_2$ , on the other hand, the FC ratio appears to be the nonresonant background level about which the oscillation in  $(v=1)/(v=0)$  varies. This may also reflect the subtle differences in the relative potential energy curves discussed above; however, we will not speculate further on this pending a direct comparison between experiment and theory in either CO or  $N_2$ .

These prototype studies are now being followed by a second wave of theoretical and experimental work aimed at broadening our perspective in this new area. As these are ongoing studies, we are only able to give a brief sketch of them at this time. A theoretical investigation<sup>28</sup> of the interaction of a  $\sigma_u$  shape resonance in  $CO_2$  (at a kinetic energy of  $\sim 18$  eV) with the symmetric-stretch mode is nearing completion. The novel aspect of that work is that nuclear motion effects practically erase evidence of this resonance in the vibrationally unresolved partial cross sections.<sup>54</sup> Nevertheless, dramatic non-Franck-Condon intensity distributions and  $v$ -dependent angular distributions are predicted<sup>28</sup> in vibrationally resolved studies. Experimental work on the "invisible"  $\sigma_u$  resonance in  $CO_2$  is beginning. Theoretical work on the  $\sigma$  resonance in CO and experimental work on the  $\sigma_u$  resonance in  $N_2$  are also underway in order to tie together the initial studies described above. Preliminary experimental results<sup>29</sup> on  $N_2$  verify all the one-electron features predicted theoretically, although significant quantitative differences are indicated. Many more case studies in this area are easily identified by looking at the recent literature on shape resonances in  $e+M$  and  $h\nu+M$  systems (see Refs. 2 and 55 for discussion of a large selection of molecules).

## ELECTRON SCATTERING RESULTS

In electron-molecule scattering the exchange of energy between a resonantly scattered electron and nuclear motion manifests itself in vibrational excitation of the target, assumed here to stay in the same electronic state. As mentioned in the Introduction, we have focussed recently on a new class of weak, intermediate-energy resonances<sup>3,45</sup> which are the counterparts<sup>30</sup> of the shape resonances in the low-energy continuum of the corresponding  $h\nu+M$  system. Here we review two examples:  $N_2$  and  $CO_2$ .

The  $N_2$  story started several years ago, when Pavlovic, Boness, Herzenberg, and Schulz<sup>46</sup> reported that "the vibrational cross section by electron impact on  $N_2$

exhibits a broad maximum near 22 eV." Prompted by the great width (FWHM > 5 eV) and the complex energy dependence of the differential cross section, those authors interpreted this enhanced vibrational excitation in terms of a large manifold of "overlapping compound states above 20 eV," including possible shape resonances and singly and multiply core-excited Feshbach resonances. Recently we proposed<sup>45</sup> a very simple, one-electron mechanism—a  $\sigma_u$  shape resonance—as a likely candidate to explain the observations of the above authors. At the very least, this resonance was shown to be responsible for enhanced vibrational excitation in the 15–35 eV range. Its ability to account for the energy dependence of the differential cross section is currently under investigation. The possible role of the  $\sigma_u$  resonance was anticipated by Pavlovic et al., but they had insufficient theoretical information to identify its primary role. This interpretation suggested itself to us during an earlier study<sup>42</sup> of e-N<sub>2</sub> scattering using the MSM with Slater exchange. That work identified weak intermediate-energy resonances in the  $\sigma_u$  and  $\delta_g$  channels, in addition to the well-known  $\pi_g$  resonance<sup>31–44</sup> at 2.4 eV. More recent work<sup>44</sup> employing the MSM with the Hara exchange approximation<sup>56</sup> has proven to be considerably superior but indicates the same three resonances, only the  $\sigma_u$  and  $\delta_g$  features are weaker, especially the  $\delta_g$ . This is consistent with recent total electron scattering measurements<sup>57</sup> on N<sub>2</sub> which indicate a very weak, broad feature at 22 eV, corresponding to the  $\sigma_u$  resonance, and no sign of the  $\delta_g$  resonance at ~13 eV. Notwithstanding the extreme weakness of these intermediate-energy features in the elastic scattering cross section, we felt they might be important in alternative scattering channels, such as vibrational excitation. Below we show that the  $\sigma_u$  is, indeed, important in this role, whereas the  $\delta_g$  is not, owing to its weakness and off-axis orientation. Results for vibrational excitation due to the strong  $\pi_g$  resonance are also presented.

Our results are shown in Figure 4. The vibrationally elastic results (0 → 0) have been discussed elsewhere.<sup>44</sup> Here we only note that although the  $\pi_g$  resonance is prominent, the bulk of the cross section is made up of nonresonant contributions. By contrast, vibrational excitation is overwhelmingly dominated by resonant processes. In Figure 4b–4d, the total cross section is indistinguishable from the resonant  $\pi_g$  (2.4 eV) and  $\sigma_u$  (26 eV) partial cross sections, indicating that nonresonant processes are negligible. Similarly, the weak  $\delta_g$  shape resonance located at ~13 eV is ineffective in enhancing vibrational excitation since it is not a strong, localized resonance (like the  $\pi_g$ ), nor an axially oriented resonance (like the  $\sigma_u$ ) and therefore couples only weakly with the nuclear motion.

Vibrational excitation via the  $\pi_g$  resonance is a well-known and often studied process;<sup>32,33,35,37,58</sup> therefore, although it is not our main focus, we will comment briefly on the comparison of these results with the earlier work. The shape of the  $\pi_g$  resonance (in vibrationally elastic and inelastic channels alike) is known<sup>35,37,38</sup> to have a vibrational substructure owing to the comparable resonance lifetime and vibrational period. Our model presently neglects such nonadiabatic effects so that we must compare our results with an average of the peaks and valleys in the experimental spectrum. Our peak values of 3.6, 1.8, and 1.0 Å<sup>2</sup> for the (0 → 1), (0 → 2), (0 → 3) transitions, respectively, agree well with an average of the vibrational substructure presented by Chandra and Temkin<sup>37</sup> and lie somewhat above experimental values, although normalization of the latter remain in doubt and could be too low by as much as a factor of two.<sup>33,37</sup>

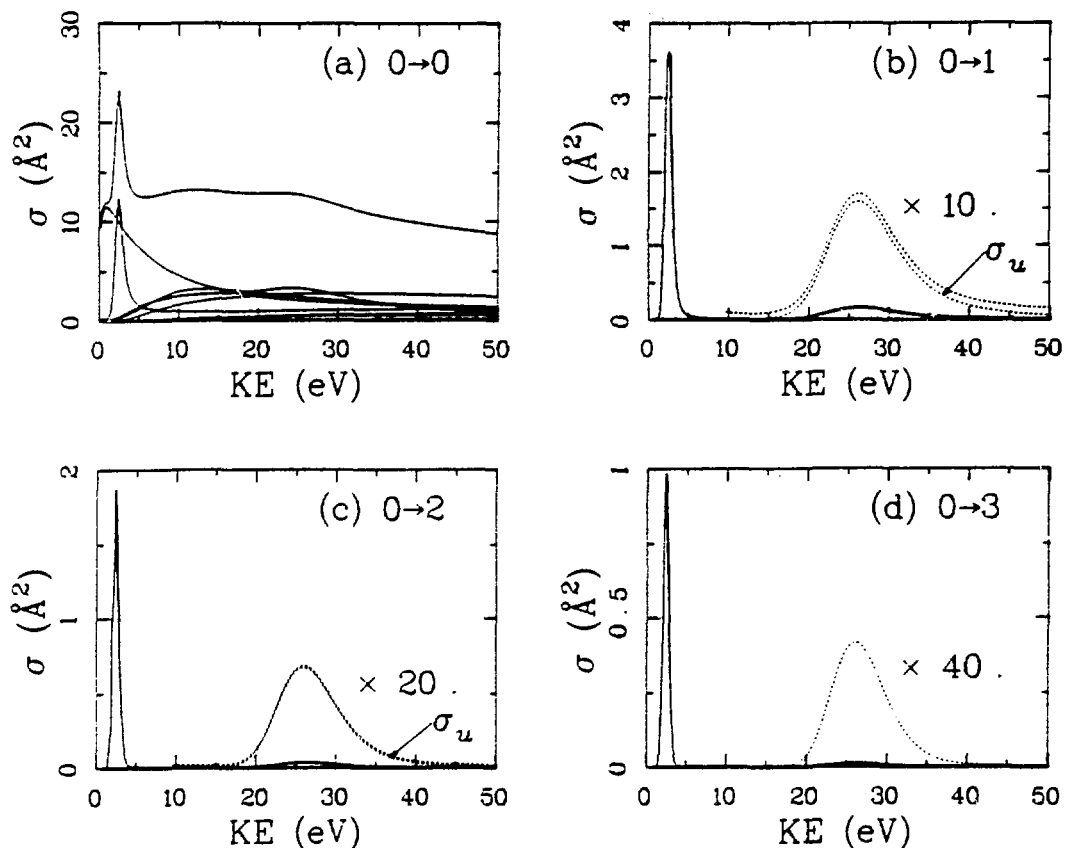


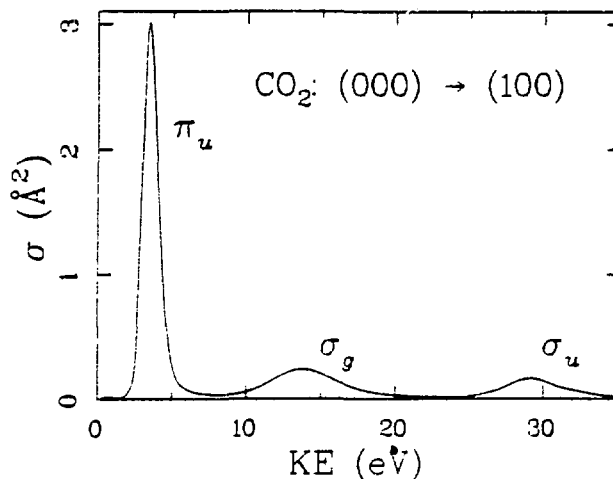
Figure 4. Vibrationally elastic and inelastic cross sections for e-N<sub>2</sub> scattering between 0–50 eV.

The other major feature in the vibrational excitation spectra between 0–50 eV is a broad hump extending from ~15 to 40 eV centered at ~26 eV. This feature is due wholly to the weak, but axially oriented  $\sigma_u$  shape resonance, and resembles the broad hump observed by Pavlovic et al.<sup>46</sup> Hence, we tentatively proposed<sup>45</sup> this simple, independent-electron mechanism as the origin of the enhanced vibrational excitation observed experimentally between 15–35 eV. Confirmation of this proposal requires further work on three questions. First, the differential cross section must be calculated for the vibrationally inelastic processes to check for the complex energy dependence observed experimentally. Second, a careful comparison of absolute magnitudes must be made. This will result from either the calculation of the differential cross section or the experimental determination of the integrated cross section for vibrational excitation. A crude estimate of the integrated cross section is given in terms of the differential cross section by  $4\pi d\sigma(90^\circ)/d\Omega$ . Using the peak values of  $d\sigma(90^\circ)/d\Omega$  reported in Ref. 33 between 15 and 35 eV, this estimate yields  $\sigma \sim 0.08 \text{ \AA}^2$  and  $0.02 \text{ \AA}^2$  for the  $v=0 \rightarrow v'=1$  and 2 channels, respectively. That these values are roughly comparable to the peak values in Figure 4 demonstrates that the  $\sigma_u$  shape resonance accounts for the bulk of the enhanced cross section in this region. Third, the discrepancy between the theoretical and experimental resonance positions is large in this case and should be resolved. Ironically, use of the Slater exchange approximation in Ref. 42 gives a resonance position of ~22 eV, in agreement with experiment, although the Hara exchange approximation is more realistic in several other respects.

The background for the e-CO<sub>2</sub> vibrational excitation calculation<sup>3</sup> is taken from MSM calculations of elastic scattering from CO<sub>2</sub> (also OCS and CS<sub>2</sub>) described in detail elsewhere:<sup>59</sup> The eigenphase sums at the equilibrium geometry for the  $\sigma$ ,  $\pi$ , and  $\delta$  scattering channels in the range 0–100 eV are given in Ref. 59. Significant rises in the eigenphase sums occur for the  $\pi_u$ ,  $\delta_g$ ,  $\sigma_g$ , and  $\sigma_u$  symmetries, at 3.4, 7, 13.5, and 29.5 eV, respectively. The low-energy  $\pi_u$  (p-wave) resonance, well-known both experimentally<sup>33,60–64</sup> and theoretically<sup>33,59,65,66</sup> stands out clearly in the integrated elastic scattering cross section. However, the higher-energy  $\delta_g$ ,  $\sigma_g$ , and  $\sigma_u$  features appear only as weak, barely noticeable, undulations on the total cross section. These undulations are further weakened when the cross section is averaged over the zero-point, symmetric-stretch oscillation of the nuclei, i. e.,  $v_i=0 \rightarrow v_f=0$  in Eq. (2).

The spectrum for excitation of the symmetric-stretch vibrational mode is shown in Figure 5. Again, the  $\pi_u$  resonance is very strong, but now the  $\sigma_g$  and  $\sigma_u$  resonances stand out clearly as well. The  $\delta_g$  resonance does not contribute appreciably since it is oriented perpendicular to the symmetric stretch and therefore is coupled weakly to it. Tronc et al.<sup>5</sup> observe the strong  $\pi_u$  induced excitation and two much weaker and broader excitations at 11 eV and 29.5 eV, with no evidence of a third ( $\delta_g$ ) weak feature, thus confirming our results. In addition, we have carried out calculations of electron scattering by OCS,<sup>59</sup> CS<sub>2</sub>,<sup>59</sup> and SF<sub>6</sub>,<sup>67</sup> and in each case high-energy shape resonances appear.

Figure 5. Cross section for excitation of the symmetric-stretch mode in CO<sub>2</sub> by electron impact.



## CONCLUSIONS

These prototype studies have demonstrated several aspects of molecular photoionization channels exhibiting shape resonances: First, the great asymmetric and non-monotonic sensitivity of the transition amplitude to internuclear separation couples the nuclear and electronic motion, invalidating the FC factorization of the two modes. This requires folding of the transition amplitude with the vibrational motion of the molecule, at the very least in an adiabatic scheme. When resonance lifetimes and the vibrational period are comparable, nonadiabatic effects (analogous to those observed<sup>33,35,37</sup> for the 2.4 eV  $\pi_g$  resonance in e-N<sub>2</sub> scattering) are likely to be important as well. Second, the effects are large in both vibrational intensities and angular distributions, but have heretofore been largely overlooked because shape resonance effects tend to lie in an inconvenient wavelength range for laboratory light sources. Synchrotron radiation will be most useful for this purpose, and we expect this to be a major theme in vibrationally

resolved photoelectron measurements using this broad-range continuum source. Third, the effects of the shape resonance described above act over tens of volts of the spectrum, several times the half-width of the resonance, and that  $\sigma$  and  $\beta$  probe the effects differently, i.e., have maximal effects in different energy regions. This underscores the well-known differences of the dynamical information contained in the two physical observables. Fourth, a long-standing "anomalous"  $\nu_f$  dependence in the photoelectron angular distributions of the  $3\sigma_g$  channel of  $N_2$  has been resolved. Finally, the phenomena described here for one channel of  $N_2$  should be very widespread, as shape resonances now appear to affect one or more inner- and outer-shell channels in most (non-hydride) molecules.

An analogous set of conclusions applies to electron-molecule scattering: First, the coupling between electronic and vibrational motion, induced by resonant scattering, enhances vibrational excitation relative to that caused by the direct scattering process. Second, this has been known for some time in the context of low-energy (0-10 eV) scattering, but has only recently been demonstrated<sup>3</sup> for intermediate-energy (10-40 eV) resonances which heretofore went undetected, since they are extremely weak in total scattering cross sections. More active investigations of these quasi-discrete states lying near the top of their potential barrier are now beginning in earnest for many molecules. Third, resonances in e+M systems demonstrate the same leverage shown by those in  $h\nu+M$  systems by translating the motion of the ground vibrational state into an effect over several volts in the spectrum. Fourth, a tentative interpretation has been provided for the enhanced vibrational excitation observed<sup>45, 46</sup> in e- $N_2$  several years ago. Finally, the pervasiveness of resonances should roughly equal that of  $h\nu+M$  systems as the two manifolds of resonances are strongly related.<sup>30</sup>

## REFERENCES

- [ 1 ] D. Dill and J. L. Dehmer, *J. Chem. Phys.* **61**, 692 (1974).
- [ 2 ] J. L. Dehmer and D. Dill, in Electron and Photon Molecule Collisions, V. McKoy, T. Rescigno, and B. Schneider, Eds. (Plenum, New York, 1979) in press.
- [ 3 ] D. Dill, J. Welch, J. L. Dehmer, and J. Siegel, *Phys. Rev. Letters*, submitted for publication.
- [ 4 ] J. L. Dehmer, D. Dill, and S. Wallace, *Phys. Rev. Letters*, submitted for publication.
- [ 5 ] M. Tronc, R. Azria, and R. Paineau, *J. de Physique Lettres*, in press.
- [ 6 ] R. Stockbauer, B. E. Cole, D. L. Ederer, J. B. West, A. C. Parr, and J. L. Dehmer, *Phys. Rev. Letters*, in press.
- [ 7 ] G. R. Wight, C. E. Brion, and M. J. van der Wiel, *J. Electron Spectrosc.* **1**, 457 (1973).
- [ 8 ] J. L. Dehmer and D. Dill, *Phys. Rev. Lett.* **35**, 213 (1975).
- [ 9 ] J. L. Dehmer and D. Dill, *J. Chem. Phys.* **65**, 5327 (1976).
- [10] J. W. Davenport, *Phys. Rev. Lett.* **36**, 945 (1976).
- [11] A. Bianconi, H. Petersen, F. C. Brown, and R. Z. Bachrach, *Phys. Rev.* **A 17**, 1907 (1978).
- [12] D. Dill, J. Siegel, and J. L. Dehmer, *J. Chem. Phys.* **65**, 3158 (1976).
- [13] J.A.R. Samson, G. N. Haddad, and J. L. Gardner, *J. Phys. B* **10**, 1749 (1977).
- [14] E. W. Plummer, T. Gustafsson, W. Gudat, and D. E. Eastman, *Phys. Rev. A* **15**, 2339 (1977).

- [15] T. N. Rescigno and P. W. Langhoff, *Chem. Phys. Lett.* 51, 65 (1977).
- [16] R. B. Kay, Ph. E. van der Leeuw, and M. J. van der Wiel, *J. Phys. B* 10, 2513 (1977).
- [17] T. N. Rescigno, C. F. Bender, B. V. McKoy, and P. W. Langhoff, *J. Chem. Phys.* 68, 970 (1978).
- [18] D. Dill, S. Wallace, J. Siegel, and J. L. Dehmer, *Phys. Rev. Lett.* 41, 1230 (1978) and 42, 411 (1979).
- [19] S. Wallace, Ph.D. Thesis, Boston University (1979).
- [20] G. V. Marr, J. M. Morton, R. M. Holmes, and D. G. McCoy, *J. Phys. B* 12, 43 (1979).
- [21] S. Wallace, D. Dill, and J. L. Dehmer, *J. Phys. B*, in press.
- [22] T. A. Carlson and A. E. Jonas, *J. Chem. Phys.* 55, 4913 (1971).
- [23] T. A. Carlson, *Chem. Phys. Lett.* 9, 23 (1971).
- [24] R. Morgenstern, A. Niehaus, and M. W. Ruf, Abstracts of Papers for the VIIth ICPEAC, July 26-30, 1971, Amsterdam, Ed., L. Branscomb et al., (North Holland, Amsterdam, 1971) p. 167.
- [25] W. H. Hancock and J.A.R. Samson, *J. Electron Spectrosc.* 9, 211 (1976).
- [26] D. M. Mintz and A. Kuppermann, *J. Chem. Phys.* 69, 3953 (1978).
- [27] R. M. Holmes and G. V. Marr, to be published.
- [28] J. R. Swanson, D. Dill, S. Wallace, and J. L. Dehmer, to be published.
- [29] J. B. West, J. L. Dehmer, A. C. Parr, R. Stockbauer, B. E. Cole, and D. Ederer, to be published.
- [30] J. L. Dehmer and D. Dill, Book of Invited Papers, Symposium on Electron-Molecule Collisions, Satellite Meeting, XI ICPEAC, University of Tokyo, Tokyo, Japan, 6-7 September 1979.
- [31] J. N. Bardsley and F. Mandl, *Reports on Progress in Physics* 31, 471 (1968).
- [32] G. J. Schulz, *Rev. Mod. Phys.* 45, 378 (1973).
- [33] G. J. Schulz, in *Principles of Laser Plasmas*, Ed., G. Bekefi (Wiley, New York, 1976) p. 33 and references therein.
- [34] M. Krauss and F. H. Mies, *Phys. Rev. A* 1, 1592 (1970).
- [35] D. T. Birtwistle and A. Herzenberg, *J. Phys. B* 4, 53 (1971).
- [36] P. G. Burke and N. Chandra, *J. Phys. B* 5, 1696 (1972).
- [37] N. Chandra and A. Temkin, *Phys. Rev. A* 13, 188 (1976).
- [38] B. D. Buckley and P. G. Burke, *J. Phys. B* 10, 725 (1977).
- [39] M. A. Morrison and B. I. Schneider, *Phys. Rev. A* 16, 1003 (1977).
- [40] M. A. Morrison and L. A. Collins, *Phys. Rev. A* 17, 918 (1978).
- [41] A. W. Fliflet, D. A. Levin, M. Ma, and V. McKoy, *Phys. Rev. A* 17, 160 (1978).
- [42] D. Dill and J. L. Dehmer, *Phys. Rev. A* 16, 1423 (1977).
- [43] J. Siegel, D. Dill, and J. L. Dehmer, *Phys. Rev. A* 17, 2106 (1978).
- [44] J. Siegel, J. L. Dehmer, and D. Dill, *Phys. Rev. A*, to be published.
- [45] J. L. Dehmer, J. Siegel, J. Welch, and D. Dill, *Phys. Rev. A*, in press.
- [46] Z. Pavlovic, M.J.W. Boness, A. Herzenberg, and G. J. Schulz, *Phys. Rev. A* 6, 676 (1972).
- [47] M. Tronc, R. Azria, and R. Paineau, to be published.
- [48] S. Wallace, D. Dill, and J. L. Dehmer, to be published.
- [49] D. M. Chase, *Phys. Rev.* 104, 838 (1956).
- [50] D. L. Albritton, private communication.
- [51] J. L. Gardner and J.A.R. Samson, *J. Electron Spectrosc.* 13, 7 (1978).
- [52] G. R. Cook, P. H. Metzger, and M. Ogawa, *Can. J. Phys.* 43, 1706 (1965).

- [53] K. Codling and A. W. Potts, *J. Phys. B* 7, 163 (1974) and references therein.
- [54] T. Gustafsson, E. W. Plummer, D. E. Eastman, and W. Gudat, *Phys. Rev. A* 17, 175 (1978).
- [55] J. L. Dehmer, *J. Chem. Phys.* 56, 4496 (1972).
- [56] S. Hara, *J. Phys. Soc. Japan* 22, 710 (1967).
- [57] R. E. Kennerly, *Phys. Rev. A*, in press.
- [58] R. K. Nesbet, *Phys. Rev. A*, to be published.
- [59] M. G. Lynch, D. Dill, J. Siegel, and J. L. Dehmer, *J. Chem. Phys.*, in press.
- [60] E. Brüche, *Ann. Phys. (Leipz.)* 83, 1065 (1927).
- [61] R. B. Brode, *Rev. Mod. Phys.* 5, 257 (1933).
- [62] C. Ramsauer, *Ann. Phys. (Leipz.)* 83, 1129 (1927).
- [63] T. W. Shyn, W. E. Sharp, and G. R. Carignan, *Phys. Rev. A* 17, 1855 (1978).
- [64] C. Szmytkowski and M. Zubek, *Chem. Phys. Lett.* 57, 105 (1978).
- [65] C. R. Claydon, G. A. Segal, and H. S. Taylor, *J. Chem. Phys.* 52, 3387 (1970).
- [66] M. Morrison, N. Lane, and L. Collins, *Phys. Rev. A* 15, 2186 (1977).
- [67] J. L. Dehmer, J. Siegel, and D. Dill, *J. Chem. Phys.* 69, 5205 (1978).